Magnetic Order in NbS_2 Nanoribbons

Francisco Güller[1,2,3], Veronica Vildosola[1,2], and Ana Maria Llois[1,2,3]

[1]Centro Atómico Constituyentes, GIyANN,CNEA, Buenos Aires, San Martín, Argentina
[2]Consejo Nacional de Investigaciones Científicas y Técnicas, Buenos Aires, Argentina
[3]Departamento de Física Juan José Giambiagi, FCEyN,UBA, Buenos Aires, Argentina

Transition metal dichalcogenides are well known for their laminar structure, similar to that of graphite. The bulk structure of many of them has been the subject of several studies during the last 30 years, due to their many potential technological applications. In the year 2004, Novoselov *et al.* achieved to isolate not only graphene but layers of other bidimensional crystals as well, among them some dichalcogenides [1]. Several metallic dichalcogenides exhibit strong Fermi surface nesting and charge density wave phases. In this contribution we study the magnetic order in NbS_2 nanoribbons, a metallic dichalcogenide, via *ab initio* calculations. We investigate the magnetization of the systems for several initial spin configurations as a function of ribbon width, comparing with results obtained for ribbons of a non metallic dichalcogenide, MoS_2. Atoms in the NbS_2 ribbons show a wave-like pattern in their magnetic moments, going from one edge to the other. The physical origin of this magnetic behavior is discussed.

***Index Terms*—Magnetic materials, magnetic moments, magnetic properties, nanostructures.**

I. Introduction

TRANSITION metal dichalcogenides are well known compounds for their layered quasi 2D structure, similar to that of graphite. The formula unit of the dichalcogenides is given by MX_2, where M denotes the transition metal (such as Mo or Nb) and X stands for S, Se or Te. Atoms within one layer are covalently bound and separate layers are held together mainly through weak Van der Waals interactions. Each layer is actually a trilayer, composed by a plane of metal atoms situated in between two planes of chalcogen atoms (X-M-X). There are two stacking possibilities (polytypes) for these layered structures, abbreviated by 1T and 2H. The 1T and 2H trilayers differ only in the relative position of the two chalcogen planes. In the 1T (2H) structure each metal atom has octahedral (trigonal prismatic) coordination. As in the case of graphene, quasi 1D structures, such as ribbons and nanotubes, can be cut out from these 2D trilayers. Different cuts produce different ribbon widths and different edge types. Nanotubes can be thought of as rolled up ribbons. The simplest edge type is the so called zig-zag one (see Fig. 1).

In 2004, Novoselov *et al.* have successfully isolated single layers of graphene and other laminar compounds, among them some transition metal dichalcogenides (TMDC) [1]. This opened the path for the investigation of the 2D and 1D structures mentioned above. So far most efforts have been concentrated on graphene, which has already revealed remarkable new phenomena and has several potential applications (see for example [2], [3]). The same can be said about graphene nanoribbons and carbon nanotubes [4], [5].

Although TDMC have received less attention, the electronic and structural properties of bulk TMDC have been widely studied in the last three decades due to their many potential technological applications. Bulk transition metal disulphides (MS_2), in general, have received special attention due to their uses in the petroleum industry as catalysts and lubricants [6], [7]. The corresponding trilayers and nanoribbons are promising candidates for applications in nanoelectronics [8], photonics [9] and tribology [10] among other fields. In particular, some of the metallic TDMC, such as 2H-$NbSe_2$ and 2H-NbS_2, show a strong nesting of the Fermi surface. This Fermi surface instability has been studied from both theoretical and experimental points of view [11], and could underlie the presence of spin density waves (SDWs), charge density waves (CDWs), superconductivity, etc. CDWs were observed for the first time in dichalcogenides approximately 35 years ago [12] and have been the subject of several studies since then [13]. 2H-NbS_2

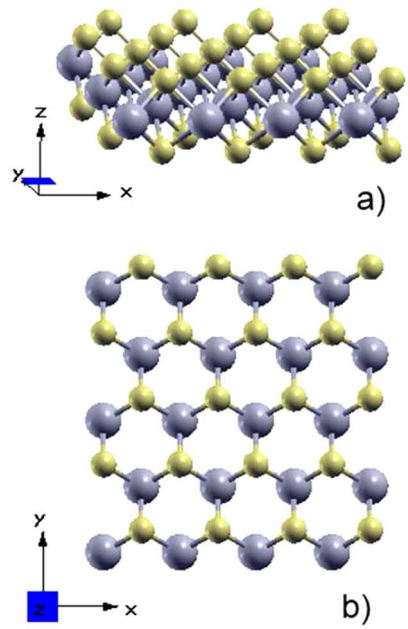

Fig. 1. Schematic representation of a zig-zag nanoribbon, as cut from a 2H trilayer (a) Side view. (b) Top view. Large spheres stand for transition metal atoms, small spheres for chalcogen atoms. The nanoribbon is periodic in the X direction.

Manuscript received February 17, 2013; revised March 28, 2013; accepted March 28, 2013. Date of current version July 23, 2013. Corresponding author: F. Güller (e-mail: guller@tandar.cnea.gov.ar).

Color versions of one or more of the figures in this paper are available online at http://ieeexplore.ieee.org.

Digital Object Identifier 10.1109/TMAG.2013.2257708

seems to be an exception in which, despite the strong nesting of the Fermi surface, no CDW or SDW state has been detected till now [14].

In this contribution we study the magnetic configurations triggered by low dimensionality in zig-zag nanoribbons of NbS_2 via *ab initio* simulations. We investigate the magnetization patterns of the systems resulting from several initial colinear spin configurations as a function of ribbon width. We compare these results with those obtained for zig-zag nanoribbons of MoS_2, a 2H type semiconductor. Nanostructures with this type of edges were realized experimentally [15], [16] and MoS_2 zig-zag nanoribbons have also been studied in previous theoretical works. They show ferromagnetic edges similar to those of graphene nanoribbons with the same edge type [17].

II. Computational Details

All calculations were performed within *ab initio* density functional theory, using the VASP [18] code. PAW pseudopotentials were used, together with the generalized gradient approximation as parameterized by Perdew *et al.* [19] for the exchange and correlation potential. Self consistent iterations were carried out until the difference in total energy between successive steps was smaller than 10^{-5} eV. The plane wave cutoff parameter was set to 550 eV and the real space projection scheme was used. The considered atomic valence configurations were $3s^2 3p^4$ for S, $4s^2 4p^6 4d^4 5s^1$ for Nb and $4s^2 4p^6 4d^5 5s^1$ for Mo. To model the infinite 1D ribbons, a supercell with a 20 Å vacuum in the two perpendicular directions was used, in order to avoid interactions between ribbons when the periodic calculations were performed. The supercell contained two primitive cells in order to allow for different initial spins and eventual dimerization. The chosen k-point grid in the corresponding first Brillouin zone was $19 \times 1 \times 1$. In relaxations, the atom positions were modified until all forces were smaller than 0.02 eV/Å.

III. Results and Discussion

NbS_2 and MoS_2 ribbons of widths between $N = 2$ and $N = 12$ were analyzed. The width, N, is defined as the number of formula units in the ribbon primitive cell. Three colinear initial magnetic configurations are considered: ferromagnetic (F), antiferromagnetic between edges (AF) and antiferromagnetic in the edge (AFE). The ferromagnetic configuration consists of having all initial spins in the same direction. In the AF configuration, all spins within one edge are aligned, but spins of atoms on different edges are opposite. In the AFE configuration, spins within one edge are alternated, but aligned between edges. In both antiferromagnetic cases, the spins of atoms away from either edge are initially set to zero. The three initial magnetic configurations are illustrated in Fig. 2. All ribbons were fully relaxed before analyzing differences arising from the different initial spin orders.

In all NbS_2 ribbons, dimerization and reduction of the lattice constant is observed upon relaxation. The effects are most noticeable on the ribbon edges and in the narrowest cases (widths 2 to 4). The lattice distortion disappears progressively as the structures become wider. The energies of the AFE state are always much higher (approximately 75 meV/primitive cell) than that of the F and AF states, showing that NbS_2 ribbon edges are ferromagnetic. Energy differences between the F and AF configurations are small, approximately 5meV/primitive cell. As an example, in Fig. 3(a), (b) and (c) we plot the magnetic moments of the individual atoms across the NbS_2 ribbons of widths 12, 11 and 10 respectively, in the lowest energy magnetic configuration obtained (AF for $N = 12$ and F for $N = 11, 10$). It can be seen that Nb atoms away from the edges of the ribbons also show a

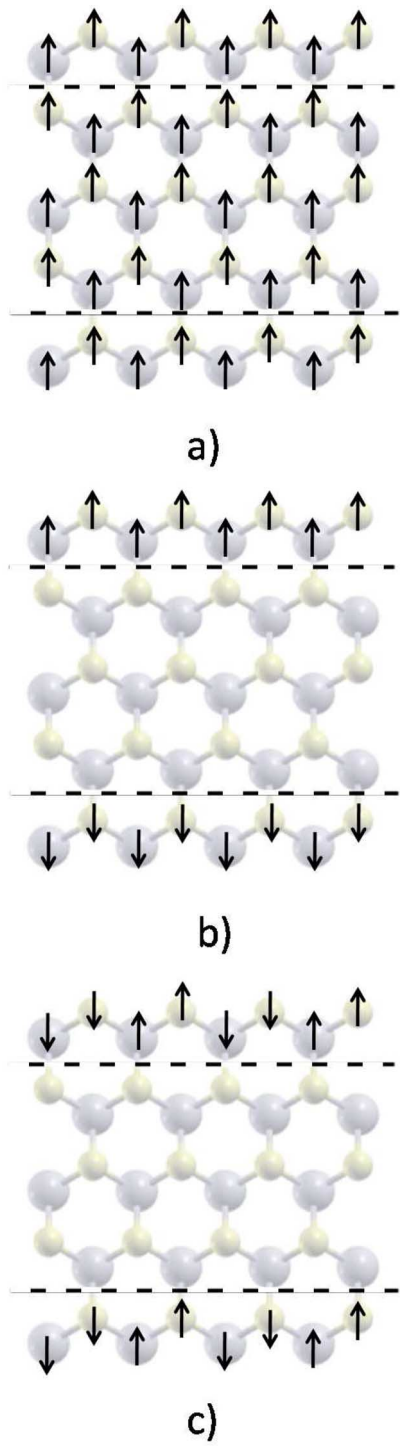

Fig. 2. Schematic representation of the initial magnetic configurations. The dashed lines separate the edge atoms of the ribbon. (a) Ferromagnetic (F), (b) antiferromagnetic (AF) and (c) antiferromagnetic between edges (AFE). Large spheres stand for Nb atoms, small spheres stand for S atoms.

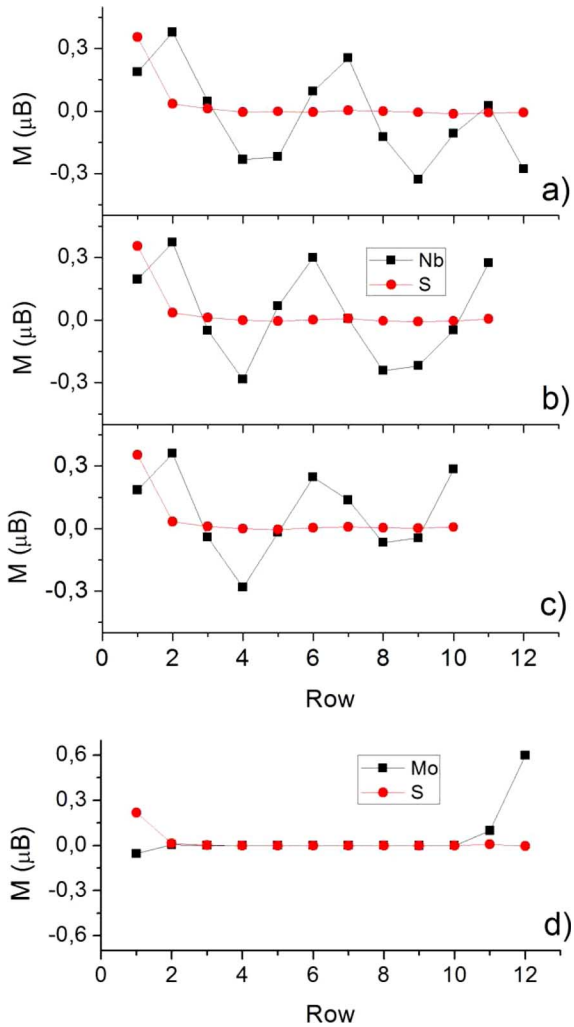

Fig. 3. Magnetic moment per atom, given row by row, for the lowest energy configuration obtained for NbS_2 ribbons of widths (a) 12 (AF), (b) 11 (F) and (c) 10 (F). (d) Magnetic moment per atom, given row by row, obtained for the MoS_2 ribbon of width 12 (F). The sulfur termination is on the left of the diagrams.

finite magnetization, while the S atoms present significant magnetization only on the S-terminated edge of the ribbons. The values of the Nb magnetic moments follow a wave-like pattern, going from one edge of the ribbon to the other. These wave-like patterns in the spins of the Nb atoms are always present, regardless of the initial magnetic configuration (AFE, AF or F). The small energy differences between the F and AF cases are due to the exchange energy required to invert the magnetic moment on the Nb-terminated edge, and break the lowest energy pattern emerging from the initial spin configurations studied.

In the MoS_2 cases, the energy difference between the AFE and F/AF configurations is similar to that on the NbS_2 ribbons. Again, the ribbon edges are ferromagnetic, as it has been reported in previous works [17]. However, energy differences between F and AF spin configurations are negligible for all widths. In contrast to NbS_2, atoms away from the edges show no magnetization (see Fig. 3(d)). The wave-like pattern of the NbS_2 ribbons magnetic moments is enabled by the existence of metallic states all across the ribbons. The MoS_2 structures, cut out from the semiconducting trilayer, have metallic states only at the ribbon edges.

We now discuss a possible physical origin behind the spin density wave-like magnetic order appearing across the NbS_2 ribbons. The amplitude of this wave does not decay across the ribbons and is of similar magnitude as the magnetic moments of the edge Nb atoms. This seems to rule out an RKKY (Ruderman-Kittel-Kasuya-Yosida) interaction between the ferromagnetic ribbon edges as the driving force behind the magnetic order of the system. This spin wave-like magnetic order could be a consequence of Fermi surface instabilities present in the 2D trilayer. The nesting of the Fermi surface, common to several dichalcogenides, results in high values of the susceptibility for specific wavevectors. These instabilities are thought to be the cause of some of the CDW phases observed in dichalcogenides such as $NbSe_2$ or TaS_2 [11], mentioned in the introduction. 2D NbS_2 trilayers in particular do not exhibit CDW or SDW [14] in spite of the high susceptibility they present for some K-vectors. A possible scenario explaining the nature of the magnetic order appearing in the NbS_2 nanoribbons, is that one dimensionality and ferromagnetic edges help to trigger the formation of low energy SDW-like states, whose origin is to be traced back to instabilities derived from important nesting at the Fermi surface of the 2D NbS_2 trilayer. The Fermi surface instabilities of the NbS_2 Fermi surface have also been addressed to explain the observed magnetic order at transition metal NbS_2 intercalates [20].

We have also observed the appearance of a wave-like magnetic order in symmetrical NbS_2 zig-zag nanoribbons (non stoichiometric) and nanoribbons with armchair edges (not shown), suggesting that the existence of this SDW-like state is not dependent on a specific ribbon edge. Also, we note that the spin orbit interaction (SOI) was not included in our calculations. However, we do not expect it to prevent the wave-like magnetic ordering which, we propose in this contribution, originates in the experimentally observed 2D Fermi surface instability [11]. Calculations of the magnetic anisotropy energy (MAE) are currently underway.

IV. Conclusion

In this contribution we calculated the magnetic properties of NbS_2 nanoribbons, a metallic TMDC, and MoS_2, a semiconductor TMDC. All ribbons have ferromagnetic edges. The NbS_2 ribbons present spin density wave-like patterns which go from one edge to the other. This magnetic order could be a consequence of the 2D Fermi surface instability, which is triggered by the ferromagnetic edge states. In the MoS_2 case, no magnetization away from the ribbon edges is observed, due to the absence of metallic states.

Acknowledgment

The authors acknowledge financial support from ANPCyT (PICT-2011-1187 and PRH074) and CONICET (PIP00273). F. G., V. V. and A. M. L. belong to the Institute of Nanoscience and Nanotechnology (INN) of the Atomic Energy Agency (CNEA), Argentina.

REFERENCES

[1] K. S. Novoselov, D. Jiang, F. Schnedin, T. J. Booth, V. V. Khotkevitch, S. Morosov, and A. K. Geim, "Two dimensional atomic crystals," *PNAS*, vol. 102, pp. 10 451–10 453, July 2005.

[2] K. S. Novoselov and A. K. Geim, "The rise of graphene," *Nature Materials*, vol. 6, pp. 183–191, July 2007.

[3] K. S. Novoselov, V. I. Falko, L. Colombo, P. R. Gellert, M. G. Schwab, and K. Kim, "A roadmap of graphene," *Nature*, vol. 490, pp. 192–200, Oct. 2012.

[4] M. F. L. D. Volder, S. H. Tawfick, R. H. Baughman, and A. J. Hart, "Carbon nanotubes: Present and future commercial applications," *Science*, vol. 339, pp. 535–539, Feb. 2013.

[5] M. Burghard, H. Klauk, and K. Kern, "Carbon-based field-effect transistors for nanoelectronics," *Adv. Mater.*, vol. 21, pp. 2586–2600, June 2009.

[6] T. A. Pecoraro and R. R. Chianelli, "Hydrodesulfurization catalysis by transition metal sulfides," *J. Catal.*, vol. 67, pp. 430–445, Feb. 1981.

[7] P. D. Fleischauer, J. R. Lince, P. A. Bertrand, and R. Bauer, "Electronic structure and lubrication properties of molybdenum disulfide: A qualitative molecular orbital approach," *Langmuir*, vol. 5, pp. 1009–1015, July 1989.

[8] B. Radisavlevic, A. Radenovic, J. Brivio, V. Giacometti, and A. Kis, "Single-layer MoS_2 transistors," *Nature Nanotech.*, vol. 6, pp. 147–150, Jan. 2011.

[9] A. Splendiani, L. Sun, Y. Zhang, T. Li, J. Kim, C. Chim, G. Galli, and F. Wang, "Emerging photoluminescence in monolayer MoS_2," *Nano. Lett.*, vol. 10, pp. 1271–1275, Mar. 2010.

[10] Z. Wu, D. Wang, Y. Wang, and A. Sun, "Preparation and tribological properties of MoS_2 nanosheets," *Adv. Eng. Mater.*, vol. 12, pp. 534–538, June 2010.

[11] D. S. Inosov, V. B. Zabolotnyy, D. V. Evtushinsky, A. A. Kordyuk, B. Büchner, R. Follath, H. Berger, and S. V. Borisenko, "Fermi surface nesting in several transition metal dichalcogenides," *New J. Phys.*, vol. 10, pp. 125027–125037, June 2008.

[12] J. A. Wilson, F. J. DiSalvo, and S. Mahajan, "Charge-density waves and superlattices in the metallic layered transition metal dichalcogenides," *Adv. Phys.*, vol. 24, pp. 117–201, Oct. 1975.

[13] K. Rossnagel, "On the origin of charge density waves in select transition-metal dichalcogenides," *J. Phys. Condens. Matter*, vol. 23, p. 213001, May 2011.

[14] M. Naito and S. Tanaka, "Electrical transport properties in 2H-NbS_2, -$NbSe_2$, -TaS_2 and -$TaSe_2$," *J. Phys. Soc. Japan*, vol. 51, pp. 219–227, Jan. 1982.

[15] K. Changki and S. P. Kelty, "Near-edge electronic structure in NbS_2," *J. Chem. Phys.*, vol. 123, pp. 24 4705–24 4711, July 2005.

[16] Z. Wang, H. Li, Z. Liu, Z. Shi, J. Lu, K. Suenaga, S.-K. Joung, T. Okazaki, Z. G. J. Zhou, Z. Gao, G. Li, S. Sanvito, E. Wang, and S. Iijima, "Mixed low-dimensional nanomaterial: 2d ultranarrow MoS_2 inorganic nanoribbons encapsulated in quasi-1d carbon nanotubes," *J. Am. Chem. Soc.*, vol. 132, pp. 13 840–13 847, Sept. 2010.

[17] H. Pan and Y. Zhang, "Edge-dependent structural, electronic and magnetic properties of MoS_2 nanoribbons," *J. Mater. Chem.*, vol. 22, pp. 7280–7290, Oct. 2012.

[18] G. Kresse and J. Furthmüller, "Efficient iterative schemes for *ab initio* total-energy calculations using a plane-wave basis set," *Phys. Rev. B*, vol. 54, pp. 11 169–11 186, Oct. 1996.

[19] J. P. Perdew, K. Burke, and M. Ernzerhof, "Generalized gradient approximation made simple," *Phys. Rev. Lett.*, vol. 77, pp. 3865–3868, Oct. 1996.

[20] C. Battaglia, H. Cercellier, L. Despont, C. Monney, M. Prester, H. Berger, L. Forr, M. G. Garnier, and P. Aebi, "Non-uniform doping across the fermi surface of NbS_2 intercalates," *Eur. Phys. J. B*, vol. 57, pp. 385–390, June 2007.